Cell Metabolism, Volume *38*

Supplemental information

Oxytocin signaling in adipocytes is required

for normal milk fat production

Erwei Li, Yangmian Yuan, Haijing Sun, Khushi Patel, Nan Zhang, Soumya Nagesh, Juan J. Aristizabal-Henao, Michael Kiebish, Christopher Jacobs, Dave Bridges, Brigid Gregg, and Evan D. Rosen

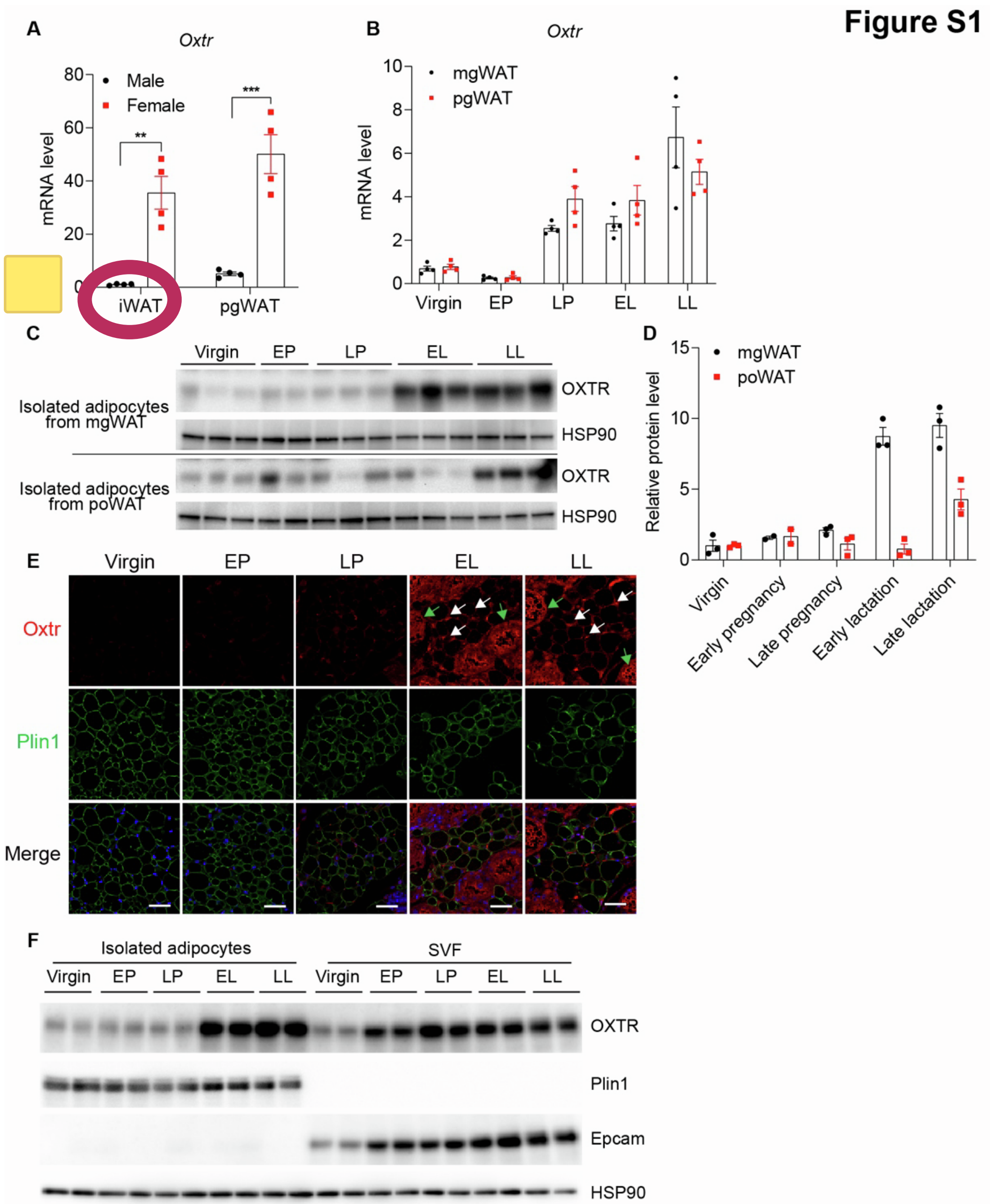

Figure S1. OXTR expression is significantly higher in female adipocytes and further increases during lactation, related to Figure 1. (A) *Oxtr* mRNA levels in male and female adipocytes from inguinal (iWAT) and perigonadal (pgWAT) white adipose tissue; n=4. **(B)** *Oxtr* mRNA levels in female adipocytes from mammary gland (mgWAT) and periovarian (poWAT) white adipose tissue across different reproductive stages, including virgin, early pregnancy, late pregnancy, early lactation and late lactation; n=4. **(C)** OXTR protein levels in female adipocytes from mgWAT and poWAT across different reproductive stages, including virgin, early pregnancy, late pregnancy, early lactation and late lactation; n=2-3. **(D)** Quantification of western blots in (C) based on densitometry. **(E)** Representative images of mgWAT of WT female mice across different reproductive stages immunostained for PLIN1 and OXTR. Green arrows indicate OXTR signals on mammary epithelial cells and white arrows indicate OXTR signals on adipocytes. Scale bars, 50um. **(F)** Western blot analysis of OXTR, PLIN1 and EPCAM in isolated adipocytes and stromal vascular fraction from mgWAT of mice at virgin, early pregnancy (EP), late pregnancy (LP), early lactation (EL), and late lactation (LL) stages; n=2.Data are presented as mean ± s.e.m. Statistical comparisons were made using 2-tailed Student's t test (A). $^{**}P < 0.01$; $^{***}P < 0.001$.

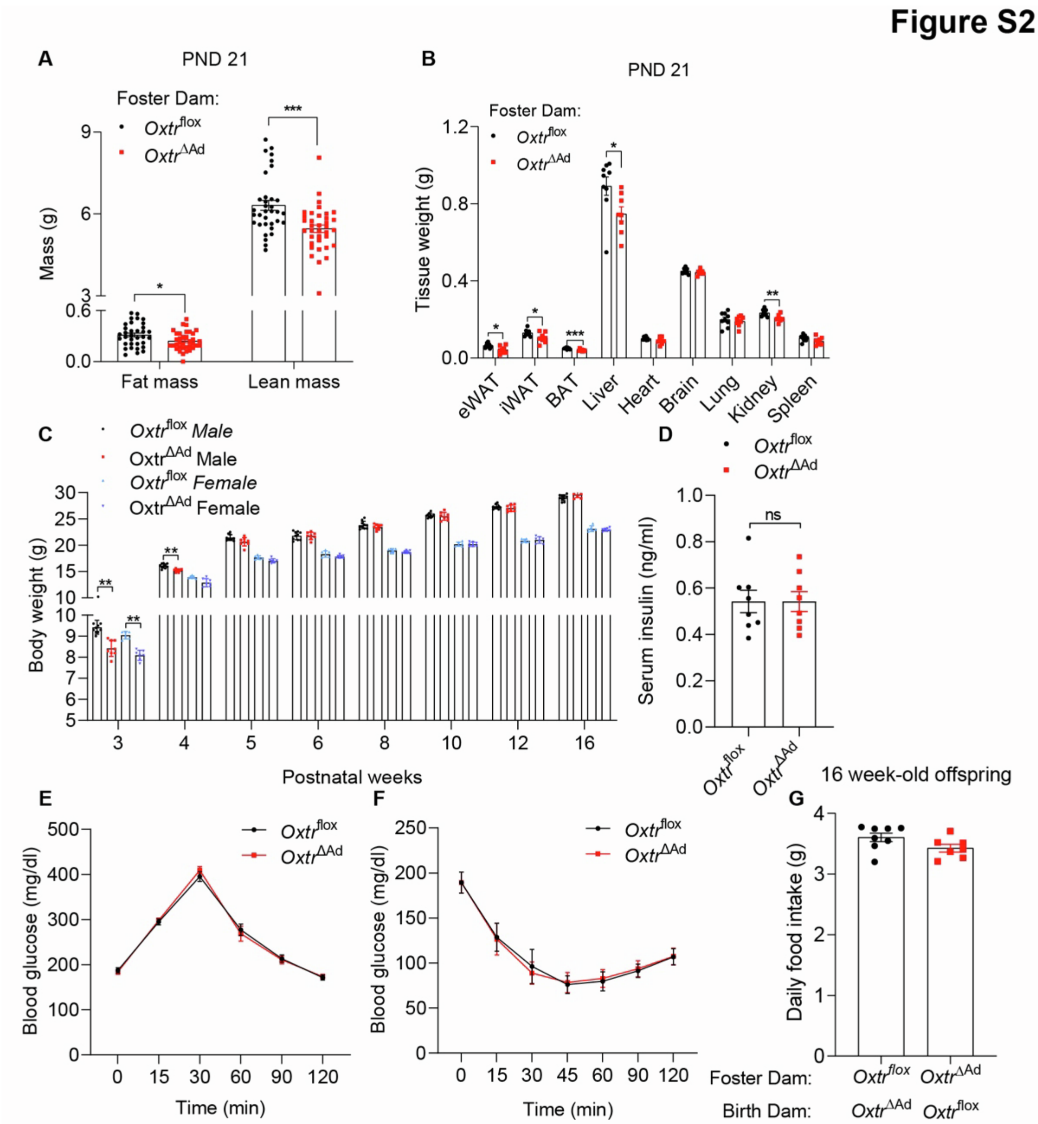

Figure S2. The phenotype of pups is determined by the genotype of dams, related to Figure 2. (A) Fat mass and lean mass of fostered pups on postnatal day 21; n=34-36. **(B)** Tissue weight of fostered pups on postnatal day 21; n=8-9. **(C)** Body weight of male and female pups of *Oxtr*^{flox} and *Oxtr*$^{\Delta Ad}$ dams at postnatal weeks 3, 4, 5, 6, 8, 10, 12, 16; n=6-10. **(D)** Serum insulin levels of 10-week-old male offspring of *Oxtr*^{flox} and *Oxtr*$^{\Delta Ad}$ dams; n=8. **(E)** GTT in 10-week-old male offspring of *Oxtr*^{flox} and *Oxtr*$^{\Delta Ad}$ dams; n=8. **(F)** ITT in 10-week-old male offspring of *Oxtr*^{flox} and *Oxtr*$^{\Delta Ad}$ dams; n=8. **(G)** Food intake of fostered mice after weaning (16 weeks old); n=7-8. Data are presented as mean ± s.e.m. Statistical comparisons were made using 2-tailed Student's t test (A-C). *P < 0.05; **P < 0.01; ***P < 0.001.

Figure S3

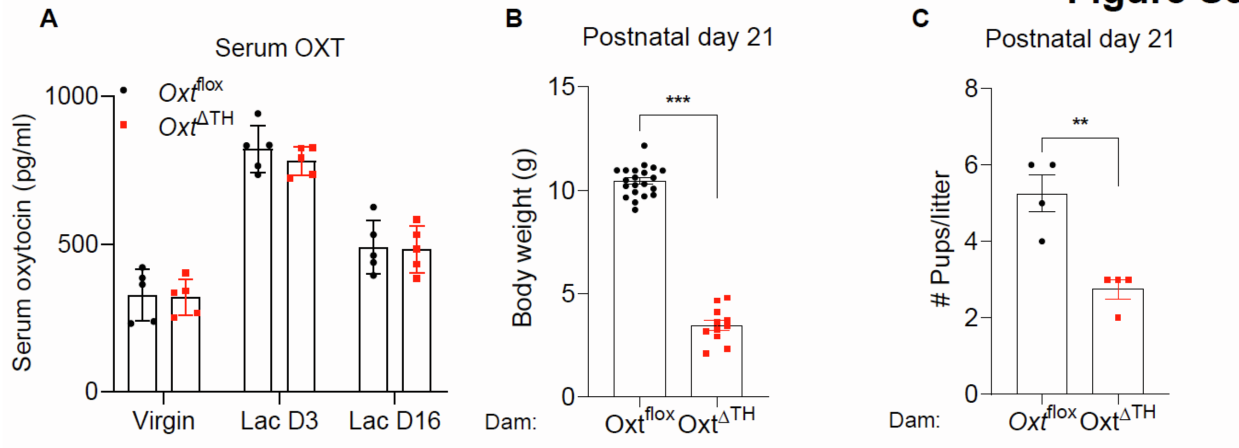

Figure S3. Pups of *Oxt*$^{\Delta TH}$ dams display impaired development during lactation, related to Figure 2. **(A)** Serum oxytocin levels in female *Oxtr*^{flox} and *Oxtr*$^{\Delta Ad}$ mice at stages of virgin, lactation day 3 and lactation day 16; n=5. **(B)** Quantification of body weight of pups from *Oxt*^{flox} and *Oxt*$^{\Delta TH}$ dams on postnatal day 21; pups of *Oxt*^{flox} dams n=21, pups of *Oxt*$^{\Delta TH}$ dams n=11. **(C)** Number of pups per litter from *Oxt*^{flox} and *Oxt*$^{\Delta TH}$ dams that survived through postnatal day 21; litters of *Oxt*^{flox} dams n=4, litters of *Oxt*$^{\Delta TH}$ dams n=4. Data are presented as mean ± s.e.m. Statistical comparisons were made using 2-tailed Student's t test (B and C). $^{**}P < 0.01$; $^{***}P < 0.001$.

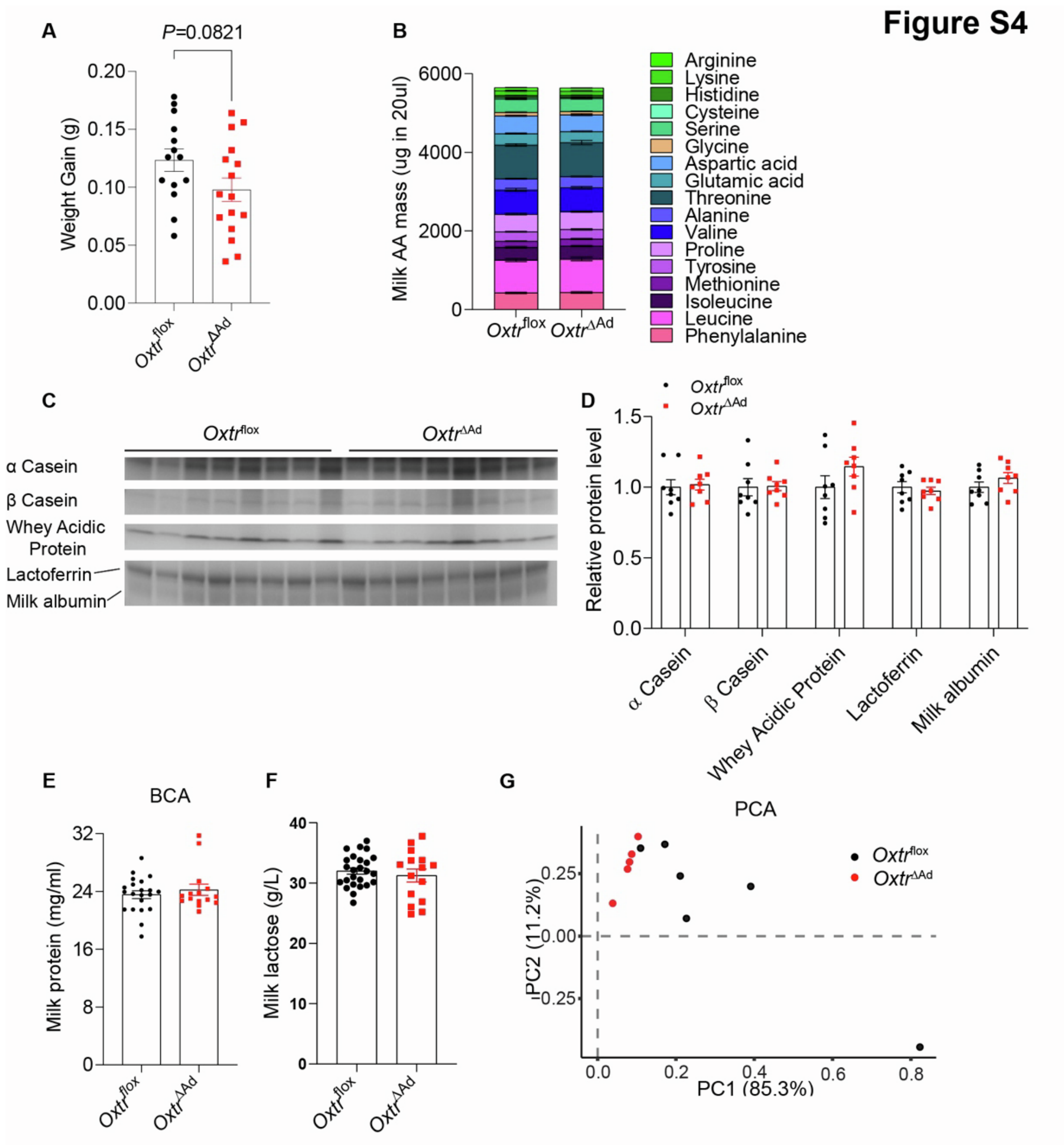

Figure S4. Milk protein and lactose levels are comparable between *Oxtr*^{flox} and *Oxtr*$^{\Delta Ad}$ dams, related to Figure 3. (A) Volume of milk produced within 3 hours by lactating *Oxtr*^{flox} and *Oxtr*$^{\Delta Ad}$ dams on postnatal day 10, measured using weigh-suckle-weigh assays; n=14-16. **(B)** Stacked plot showing the mass distribution of total amino acids in milk samples from *Oxtr*^{flox} and *Oxtr*$^{\Delta Ad}$ dams on postnatal day 16; n=6. **(C)** Protein levels of α casein, β casein, whey acidic protein, lactoferrin and albumin in milk samples collected from *Oxtr*^{flox} and *Oxtr*$^{\Delta Ad}$ dams on postnatal day 16; n=8. **(D)** Quantification of (D) based on densitometry. **(E)** Total protein levels in milk collected from lactating *Oxtr*^{flox} and *Oxtr*$^{\Delta Ad}$ dams, n=15-21. **(F)** Lactose levels in milk collected from *Oxtr*^{flox} and *Oxtr*$^{\Delta Ad}$ dams on postnatal day 16; n=15-25. **(G)** PCA of lipids from milk samples of *Oxtr*^{flox} and *Oxtr*$^{\Delta Ad}$ dams on postnatal day 16. Each dot indicates an individual biological replicate; n=5. Data are presented as mean ± s.e.m. Statistical comparisons were made using 2-tailed Student's t test (A and D-F).

Figure S5

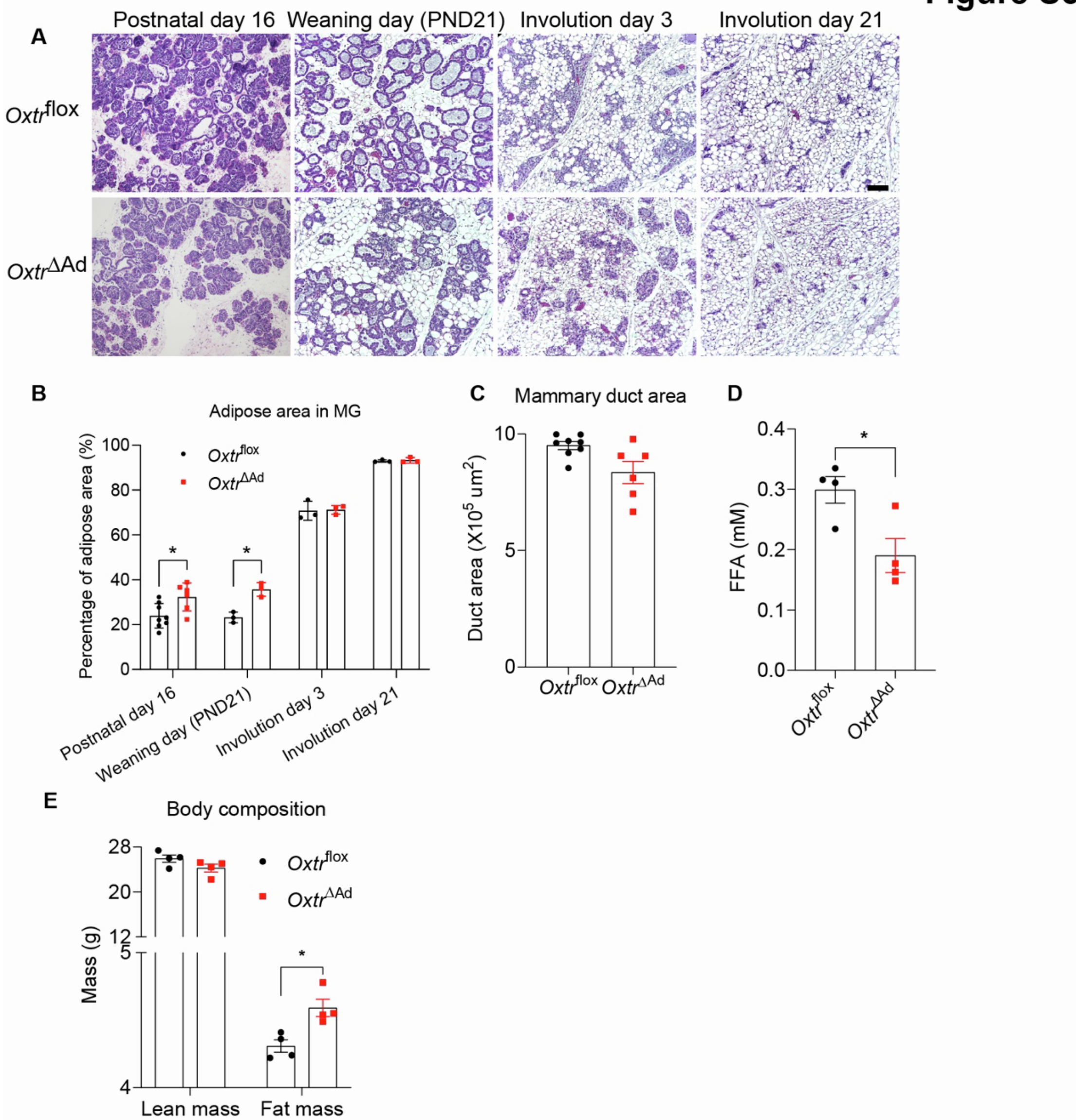

Figure S5. More fat is reserved in lactating *Oxtr*$^{\Delta Ad}$ dams, related to Figure 3. (A) Representative histology sections of mammary glands dissected from *Oxtr*^{flox} and *Oxtr*$^{\Delta Ad}$ dams on postnatal day 16, weaning day (PND21), involution day 3 and involution day 21. **(B)** Quantification of adipose area in mammary gland sections from *Oxtr*^{flox} and *Oxtr*$^{\Delta Ad}$ dams on postnatal day 16, weaning day (PND21), involution day 3 and involution day 21; n=6-8. **(C)** Quantification of duct area in mammary gland sections from *Oxtr*^{flox} and *Oxtr*$^{\Delta Ad}$ dams on postnatal day 16; n=6-8. **(D)** Serum free fatty acid levels in lactating *Oxtr*^{flox} and *Oxtr*$^{\Delta Ad}$ dams on postnatal day 11; n=4. **(E)** Body composition of lactating *Oxtr*^{flox} and *Oxtr*$^{\Delta Ad}$ dams on postnatal day 10; n=4. Data are presented as mean ± s.e.m. Statistical comparisons were made using 2-tailed Student's t test (B-E). *P < 0.05.

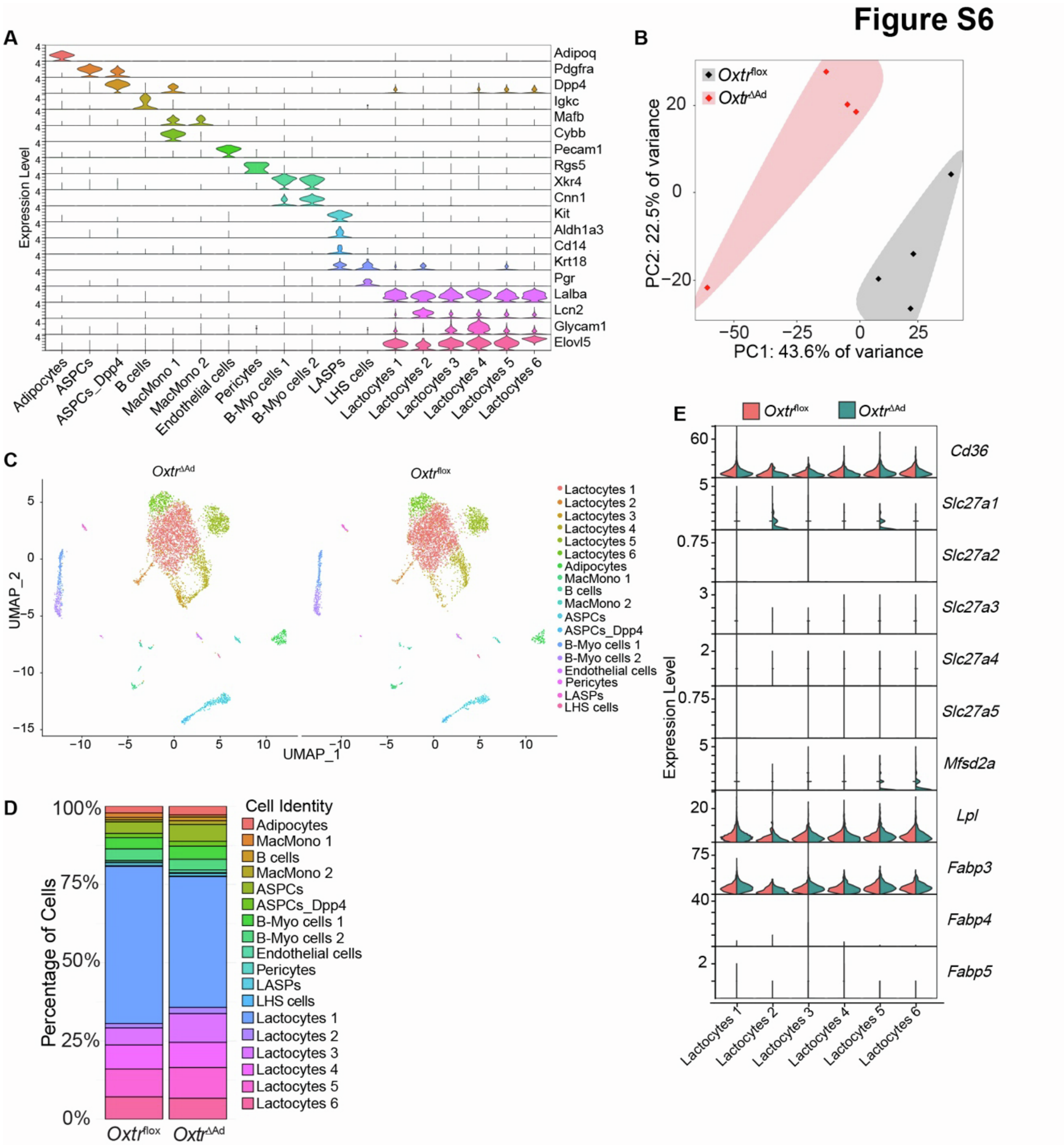

Figure S6. The proportions of each cell type within the mammary glands are comparable between *Oxtr*^{flox} and *Oxtr*$^{\Delta Ad}$ dams, related to Figure 4. (A) Marker genes for each cell type in lactating mammary glands from *Oxtr*^{flox} and *Oxtr*$^{\Delta Ad}$ dams. **(B)** PCA of pseudo-bulk single cell RNA-seq data of mammary glands showing cluster formation of lactocytes between *Oxtr*^{flox} and *Oxtr*$^{\Delta Ad}$ dams. **(C)** UMAP projection of all 13,035 sequenced mammary gland nuclei split by genotype. **(D)** Stacked plot showing the proportions of each cell type in mammary glands from lactating *Oxtr*^{flox} and *Oxtr*$^{\Delta Ad}$ dams on postnatal day 11. **(E)** Stacked violin plot showing the expression of genes related to lipid transport and uptake in lactocytes of *Oxtr*^{flox} and *Oxtr*$^{\Delta Ad}$ dams.

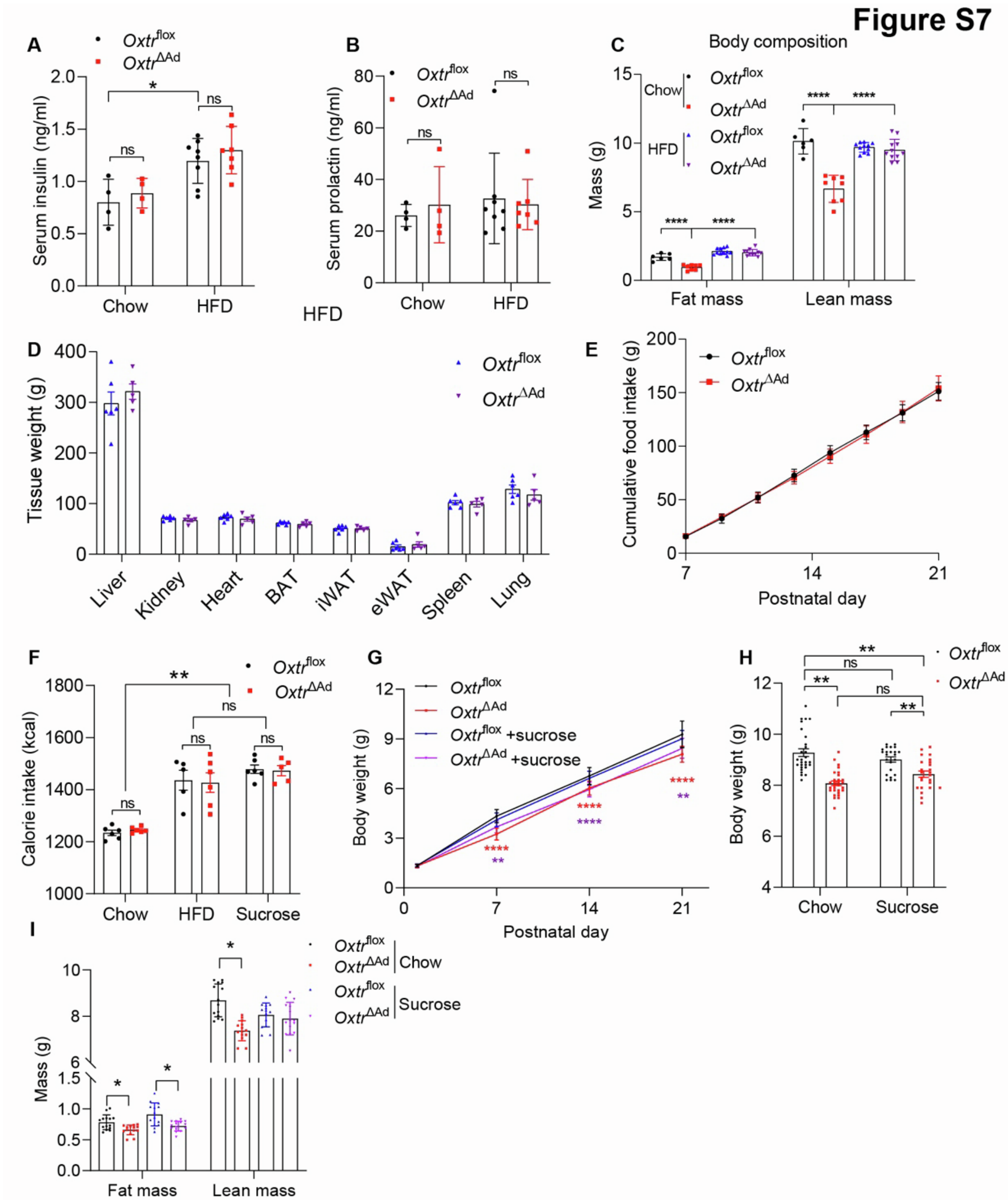

Figure S7. Dietary lipid supplementation rescues the developmental phenotype of pups of *Oxtr*$^{\Delta Ad}$ dams, related to Figure 5. (A) Serum insulin levels in *Oxtr*^{flox} and *Oxtr*$^{\Delta Ad}$ dams on either chow or HFD; n=4-8. **(B)** Serum prolactin levels in *Oxtr*^{flox} and *Oxtr*$^{\Delta Ad}$ dams on either chow or HFD; n=4-8. **(C)** Body composition of pups of *Oxtr*^{flox} and *Oxtr*$^{\Delta Ad}$ dams on chow or HFD on postnatal day 21; n=6-8. **(D)** Tissue weight of pups of *Oxtr*^{flox} and *Oxtr*$^{\Delta Ad}$ dams on HFD on postnatal day 21; n=5-6. **(E)** Cumulative food intake of *Oxtr*^{flox} and *Oxtr*$^{\Delta Ad}$ dams during lactation; n=4-6. **(F)** Accumulated calorie intake of *Oxtr*^{flox} and *Oxtr*$^{\Delta Ad}$ dams on chow, HFD or chow plus *ad libitum* sucrose water during lactation; n=5-6. **(G)** Body weight of pups from *Oxtr*^{flox} and *Oxtr*$^{\Delta Ad}$ dams either on chow or chow plus *ad libitum* sucrose water during lactation; n=23-30. **(H)** Body weight of pups of *Oxtr*^{flox} and *Oxtr*$^{\Delta Ad}$ dams either on chow or chow plus *ad libitum* sucrose water during lactation on postnatal day 21; n=23-29. **(I)** Body composition of pups of *Oxtr*^{flox} and *Oxtr*$^{\Delta Ad}$ dams either on chow or chow plus *ad libitum* sucrose water during lactation on postnatal day 21; n=14-15. Data are presented as mean ± s.e.m. Statistical comparisons were made using 2-tailed Student's t test (A, B, D-F, H, and I) or 2-way ANOVA (C and G). ****P<0.0001.